THE JOURNAL OF PHYSICAL CHEMISTRY C

ARTICLE

pubs.acs.org/JPCC

^{6}Li 1D EXSY NMR Spectroscopy: A New Tool for Studying Lithium Dynamics in Paramagnetic Materials Applied to Monoclinic Li_2VPO_4F

L. J. M. Davis,[†] B. L. Ellis,[‡] T. N. Ramesh,[‡] L. F. Nazar,[‡] A. D. Bain,[†] and G. R. Goward*[,†]

[†]McMaster University, Department of Chemistry and Chemical Biology, 1280 Main Street, West Hamilton, ON, L8S 4M1 Canada

[‡]University of Waterloo, Department of Chemistry, 200 University Avenue West, Waterloo, Ontario, N2L 3G1, Canada

ABSTRACT: ^{6}Li selective inversion NMR studies are used to probe details of Li mobility in Li_2VPO_4F. Two crystallographically unique Li sites were resolved under magic-angle spinning (25−40 kHz) with paramagnetic shifts arising at 46 and −47 ppm (330 K). The rate of exchange between these sites was evaluated using selective inversion (or one-dimensional exchange (1D EXSY)) NMR. This methodology relies on relaxation-based experiments that provide a means for mobility time scales to be determined for materials in which Li^+ ions exchange slowly relative to their T_1 spin−lattice relaxation. This situation is particularly relevant to cathode materials for lithium ion batteries, where the unpaired electrons of the transition-metal centers provide a dominant mechanism for rapid relaxation. In Li_2VPO_4F, Li1−Li2 exchange pair jump rates extend from 24 (±1) to 55 (±4) Hz over a temperature range of 330−350 K. The activation energy for this ion exchange process was measured to be 0.44 (±0.06) eV.

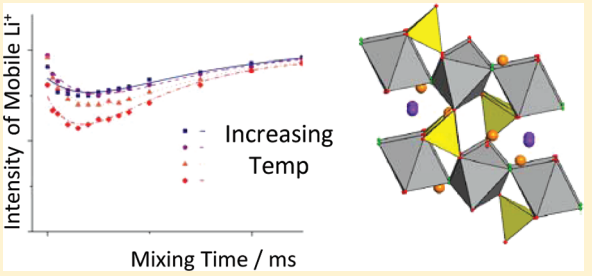

INTRODUCTION

There has been significant effort in recent years to improve the performance of Li-ion batteries to enable their realization in automotive applications. For this goal to be achieved, the cost, lifetime, and safety issues of current Li-ion battery technology need to be addressed.[1,2] This has led to widespread investigation into replacement of the many chemical components in Li-ion batteries currently used in electronic devices. For the positive electrode material, many new intercalation compounds have been introduced based on phosphates and more recently fluorophosphates.[3] These newer cathodes show impressive cycling capabilities and are typically environmentally benign and economically accessible. With these new materials, however, to better understand cycling failure, successes, or both, the behavior of the mobile ion must be understood. Whereas powder X-ray diffraction as well as a variety of other spectroscopic techniques can provide useful information about structural changes to the lattice taking place during chemical/electrochemical cycling, very few techniques can directly monitor the mobile ion. Solid-state ^{6,7}Li nuclear magnetic resonance (NMR) is one of these few techniques and can provide time scales and activation energies for Li-ion mobility.

Here we utilize MAS NMR methods to quantify mobility time scales in monoclinic Li_2VPO_4F. The oxidized form of this compound is the tavorite-based $LiVPO_4F$, which was first reported by Barker et al. as a high capacity (155 mAh/g) 4.1 V positive electrode material for Li-ion batteries.[4] Recent studies have characterized the structure and electrochemical properties of the reduced phase, Li_2VPO_4F, where intercalation of the second lithium environment takes place with a $V^{3+}-V^{2+}$ redox potential of 1.8 V.[5] This structure is proposed to have 3D conduction pathways[5] which are considerably advantageous over more well-known cathode materials including olivine $LiFePO_4$, which is restricted to 1D tunnels for conduction.[6] Here we evaluate the behavior of the mobile ion and determine the propensity for 3D diffusion within the reduced phase.

Previous studies have used 2D ^{6,7}Li exchange spectroscopy (2D EXSY)[7] as a means to understand and quantify time scales of Li-ion exchange of intercalation materials that include Li_4SiO_4,[8] $LiMn_2O_4$,[9] $Li_3M_2(PO_4)_3$ (M = V, Fe),[10,11] and more recently Li_3VF_6.[12] In these studies, the buildup of cross peak volume as a function of mixing time is monitored, and the correlation time (τ_c) of an exchange process is determined. This experiment is simplified when the correlation time of the exchange process is sufficiently shorter than the relaxation times of the nuclei being measured. This condition is not normally met in the ^{6,7}Li MAS NMR of many Li-ion cathode materials where the redox active center is typically paramagnetic. The very strong through-bond and through-space couplings of the NMR active nuclei with the unpaired electrons at the transition-metal leads to broad resonances that have short spin−lattice relaxation times (T_1) and spin−spin relaxation times (T_2). The short T_1 times, while advantageous from the standpoint of signal averaging over many scans, can make analysis of the ^{6,7}Li 2D EXSY nontrivial.[13] Therefore, in the present study, a simpler and more experimentally efficient method for determining the kinetics of lithium ion dynamics in a Li-intercalation material is used, where the effects

Received: June 24, 2011
Revised: September 21, 2011
Published: September 22, 2011

dx.doi.org/10.1021/jp2059408 | J. Phys. Chem. C 2011, 115, 22603–22608

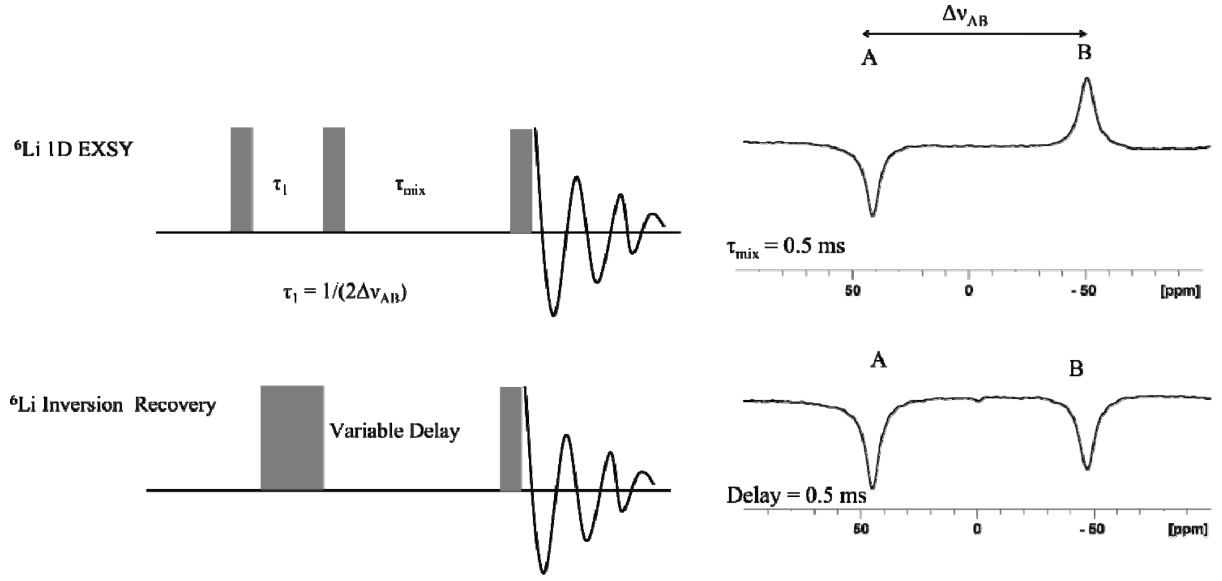

Figure 1. Top: Pulse sequence for 1D ^{6}Li MAS EXSY experiments along with sample spectrum at short τ_{mix}. The 90-τ_1-90 portion allows for selective inversion of the A site (which is the on resonance spin). The first delay period (τ_1) is defined as $1/(2\Delta\nu_{AB})$. The second delay period is the mixing time that is stepped over a series of experiments. Bottom: a nonselective, inversion recovery standard pulse sequence with sample spectrum obtained with a short delay time. The delay time is stepped in an identical manner to the mixing time of the 1D EXSY experiment.

of both chemical exchange and spin−lattice relaxation are quantitatively considered.[14,15]

^{6}Li 1D EXSY Experiments. Measurement of ion dynamics in Li_2VPO_4F was accomplished using one-dimensional exchange spectroscopy (1D EXSY) experiments. This relaxation-type experiment selectively inverts a spin undergoing ion exchange and monitors the return to equilibrium as a function of time. (In this study, it is termed the mixing time, τ_{mix}.)[14−17] In a multispin system, for the selectively inverted spin (i), the relaxation (R_i) is composed of the inherent T_{1i} time as well as the sum of the rate constants (k) associated with each exchange process that is taking place with spin (i) (eq 1)[18]

$$R_i = \frac{1}{T_{1i}} + \sum_{i \neq j} k_{ij} \qquad (1)$$

Conversely, the noninverted spin(s) will experience an attenuation of signal intensity as a function of mixing time during the period where chemical exchange is taking place. This results in a characteristic "transient" curve for the noninverted spin, which, if accurately modeled, yields kinetic information. By modeling the experimental data, an accurate and quantitative determination of exchange time scales is achieved.[14,15,19−21] Figure 1 shows that the pulse sequence used in this study for selective inversion of the on-resonance A spin. These experiments use a simple 90°−τ_1−90°−τ_{mix}−90° sequence, where τ_1 is set equal to $1/(2\Delta\nu_{AB})$ with $\Delta\nu_{AB}$ being the frequency difference between the A and B resonances. The mixing time (τ_{mix}) is stepped over a series of experiments such that the time scales of ion exchange can be determined. Nonselective inversion recovery experiments are also utilized to illustrate how ion exchange rates are separated from inherent T_1 properties through the use of selective inversion methods.

Whereas this experimental approach has found widespread application in many liquid-state systems, as illustrated by the range of materials investigated using selective-inversion studies within the past few years alone,[22−27] selective-inversion studies in the solid state remain sparse. An initial report of solid-state 1D EXSY quantified the time scale and energy barrier of a proton hop during an interconversion process in α-tropoline.[28] Other recent examples of related solid-state NMR research utilizing the 1D EXSY method include studies of oxygen dynamics in the oxygen conductor, ZrW_2O_8, and studies of deuterium dynamics in magnesium−titanium alloys, used for hydrogen storage.[29,30]

Here we report the first solid-state selective-inversion study of a paramagnetic system, implemented to quantitatively describe the lithium ion dynamics in the cathode material, Li_2VPO_4F. This is an ideal system because it has shown slow exchange relative to the spin−lattice relaxation of both Li sites.[5] Furthermore, the baseline resolution between the two NMR spins makes it an ideal candidate for selective-inversion of one spin while leaving the other spin unperturbed.

EXPERIMENTAL SECTION

Sample Preparation. Samples of Li_2VPO_4F were prepared from stoichiometric chemical lithiation of $LiVPO_4F$. $LiVPO_4F$ was prepared according to the method reported by Barker et al.:[4] V_2O_5 (Aldrich, 99%+), $NH_4H_2PO_4$ (BDH, 99%), and carbon black were mixed in a 0.5:1:1.5 molar ratio and fired at 750 °C under a flowing Ar atmosphere to produce carbon-coated VPO_4. VPO_4 and LiF were combined in stoichiometric amounts and milled with zirconia milling media for 4−6 h. The powder was fired at 600 °C for 1 h under an Ar atmosphere to form $LiVPO_4F$. $LiVPO_4F$ was then stirred with a stoichiometric amount of $LiAlH_4$ in tetrahydrofuran in an argon-filled glovebox for 44 h. The final product, Li_2VPO_4F, was washed with tetrahydrofuran and stored under argon.

Solid-State NMR. A custom built 1.8 mm probe with MAS speed of 40 kHz was used for initial characterization at a Larmor frequency of 44.1 MHz. Variable temperature experiments were carried out using a Bruker 2.5 mm probe with MAS frequency of 25 kHz. Temperatures were calibrated using $Sm_2Sn_2O_7$, as described elsewhere.[31] ^{6}Li 1D MAS spectra were acquired with a 90° pulse of 2.5 μs and recycle delay of 200 ms.

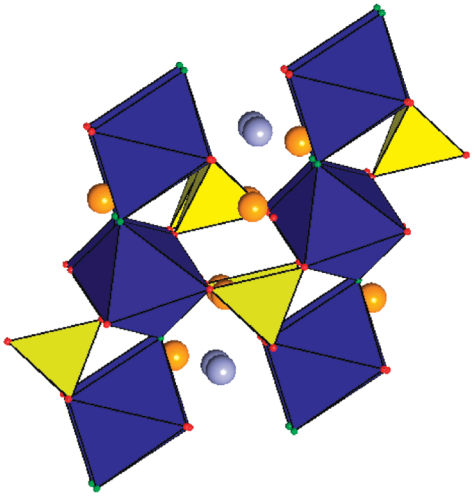

Figure 2. Structure of Li_2VPO_4F, which crystallizes in the monoclinic space group, $C\,2/c$, with lithium ions on the 8f Wyckoff positions, each with occupancy of 0.5.[31] Li1 (orange) and Li2 (lilac) sit in channels framed by corner sharing phosphate tetrahedra (yellow) and vanadium octahedra (blue).

1D ^{6}Li EXSY experiments were performed using a $90°-\tau_1-90°-\tau_{mix}-90°$ sequence, also with a 90° pulse of 2.5 μs and recycle delay of 200 ms. For our two-site system, selective inversion of the lower frequency A spin was accomplished using a 90° pulse, set on resonance to spin A. During the first $[90°-\tau_1-90°]$ portion of the sequence, where τ_1 is set to $1/(2\Delta\nu_{AB})$, the on-resonance spin is selectively inverted following the second 90° pulse. Mixing times (τ_{mix}) were stepped over a series of 16 experiments from 5 μs to 100 ms (the latter delay time being well beyond the relaxation rates of both spins to ensure that both spins had magnetization measured at equilibrium). Non-selective inversion (NSI) experiments were performed using the standard inversion–recovery sequence. The same variable delay list was used in the NSI, as was used in the 1D EXSY experiments. In both the SI and NSI studies, a digital filter was applied to allow for acquisition and analysis of the centerband region only.

Data Analysis. In each data set, slices for each mixing time/variable delay were extracted and baseline-corrected. After integration of both spins involved in the exchange process, these values were normalized to the integration value of the slice collected at the longest mixing time/variable delay (where the magnetization of each spin was fully relaxed). The data were fit using the CIFIT program developed by Bain et al.[18] This program utilizes a table of observed intensities for all spins as a function of mixing time and determines a key set of parameters: the jump rates (k) of each chemical exchange process, spin–lattice relaxation times in the absence of chemical exchange (T_1), and the magnetization values from initial to equilibrium conditions (i.e., from $M_i(0)$ to $M_i(\infty)$). The rate matrix used to describe spin relaxation under the influence of chemical exchange is the primary mathematical model used by the CIFIT program and is described in greater detail elsewhere.[18,21,32] CIFIT adjusts the free parameters, T_1, k, $M_i(0)$, and $M_i(\infty)$ until the sum of the squares of the differences between the experimental and calculated data is minimized. Error values of the exchange rates were approximated in the CIFIT program by the variance–covariance matrix of the fit to the data.[18]

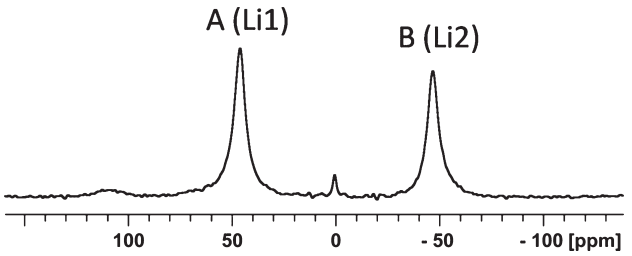

Figure 3. – ^{6}Li MAS NMR spectrum of Li_2VPO_4F with MAS = 40 kHz. The two crystallographic sites are labeled accordingly.

Table 1. Summary of Exchange Rates and Correlation Times from ^{6}Li EXSY Studies of Li_2VPO_4F

temperature (K)	exchange rate (Hz)	correlation time (ms)
331 K	24 (±1)	41 (±2)
337 K	30 (±1)	34 (±1)
343 K	40 (±2)	25 (±1)
350 K	55 (±4)	18 (±1)
activation energy	0.44 (±0.06) eV	

RESULTS AND DISCUSSION

The two Li crystallographic positions in Li_2VPO_4F (Figure 2)[5] were resolved in the 1D ^{6}Li NMR spectrum with MAS of 40 kHz (Figure 3). Resonances centered at 46 and −47 ppm are assigned as sites A and B. There is a small diamagnetic impurity centered at 0 ppm, which is not involved in the exchange process and therefore omitted from the analysis. The high-frequency resonance centered at ∼112 ppm belongs to the parent $LiVPO_4F$ and results from incomplete lithiation. It constitutes <4% of the total signal when integrated across the entire sideband manifold. Spin–lattice relaxation (T_1) times of both resonances were determined at room temperature using a nonselective inversion recovery experiment. Site A has a spin–lattice relaxation time of 23 (±1) ms and site B has a spin–lattice relaxation time of 18 (±1 ms).

Our previous investigations confirmed the lithium ion dynamics within the Li_2VPO_4F, using a qualitative 2D EXSY experiment, where the expected cross peaks were observed for the doubly lithiated phase, whereas no cross peak between the doubly and singly lithiated phases was detected, confirming the two-phase nature of the lithiation process.[5] To determine the time scales and energy barriers of exchange in the doubly lithiated phase, ^{6}Li 1D EXSY experiments were applied over a variable temperature range. For the two-spin system, Li_2VPO_4F, resonance A was chosen for inversion, whereas resonance B was left unperturbed. Data collected from ^{6}Li 1D EXSY experiments over a variable temperature range are shown in Figure 4a. At all temperatures, the strong buildup of the inverted A spin is accompanied by a transient "well" in the intensity of the B spin. This clearly shows the expected chemical exchange taking place between the two sites. The effect of temperature, on both the buildup of the A spin as well as the transient well of the B spin, is better illustrated in Figure 4b. Here the A and B curves are separated and then each plotted over the entire temperature range. This x axis has been adjusted to show the shorter mixing times where the influence of the ion dynamics is more prominent. The lines drawn show the best fit to the data from the CIFIT program. Results of the CIFIT program are shown in Table 1.

dx.doi.org/10.1021/jp2059408 |J. Phys. Chem. C 2011, 115, 22603–22608

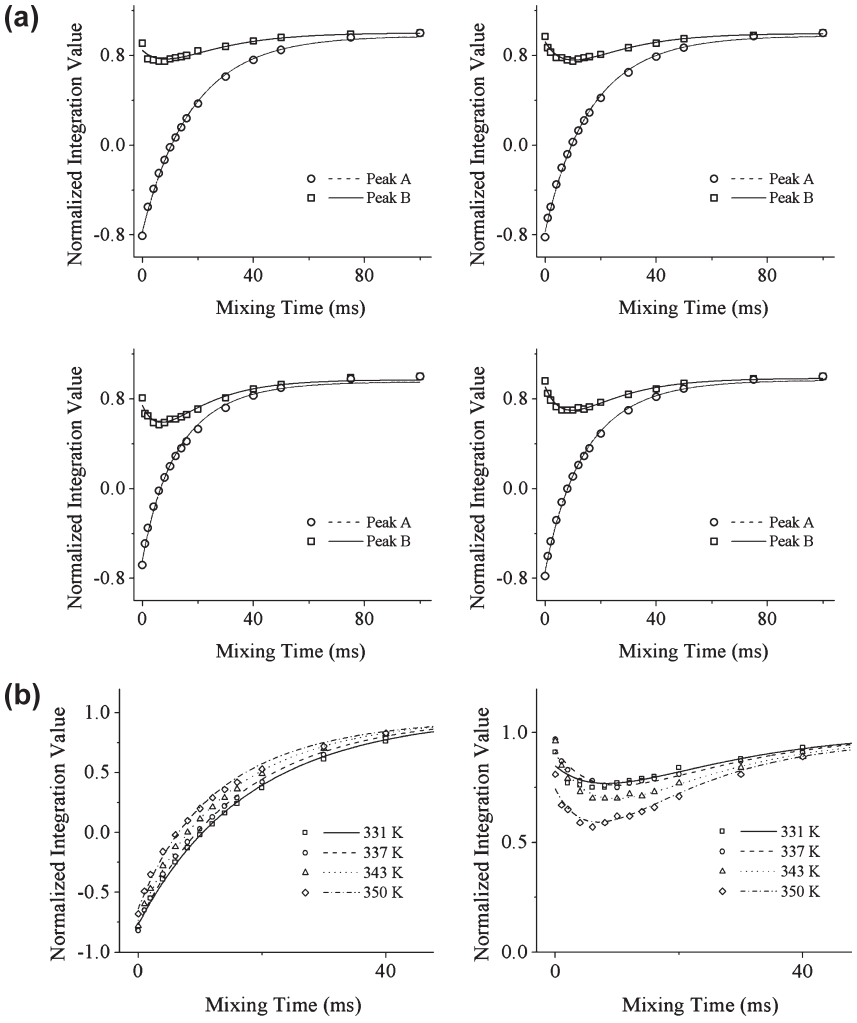

Figure 4. (a) Results of the ^{6}Li 1D EXSY experiments over a variable temperature range. Clockwise from the top left, 331, 337, 343, and 350 K. The points represent measured values, and the lines are the best fit to the data from the CIFIT program. The depth of the transient well increases with increasing temperature. (b) Results of the ^{6}Li 1D EXSY experiments over a variable temperature range. Plots are separated into the inverted A spin (left) and non-inverted B spin (right). Data points represent measured values, and the lines are the best fit to the data from the CIFIT program.

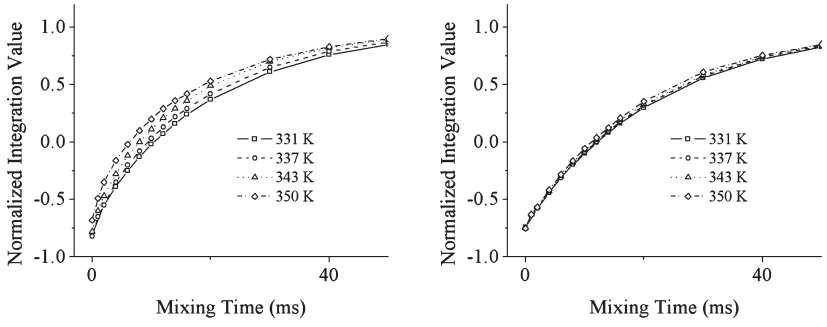

Figure 5. Results of selective 1D ^{6}Li EXSY (left) and nonselective inversion (NSI) recovery (right) experiments of the A resonance over the same temperature range. The *x* axis is minimized to the time region where chemical exchange is expected to dominate the buildup curves. The 1D EXSY results show an increase in buildup intensity as the temperature is raised. The NSI recovery shows only a slight variation with temperature.

As the temperature is increased from 331 to 350 K, the exchange rate is increased from 24 ± 1 to 55 ± 4 Hz. The lower limit of the temperature range in this experiment was governed by the ion dynamics of this material, where no exchange was observed at temperatures below 330 K. The upper limit of the temperature range was governed by the instrumentation, where 350 K was the highest possible temperature for the probe.

The effectiveness of ^{6}Li 1D EXSY experiments in separating rate information from inherent T_1 properties is demonstrated in Figure 5. Here ^{6}Li 1D NSI experiments, recorded over the same

dx.doi.org/10.1021/jp2059408 |*J. Phys. Chem. C* 2011, 115, 22603–22608

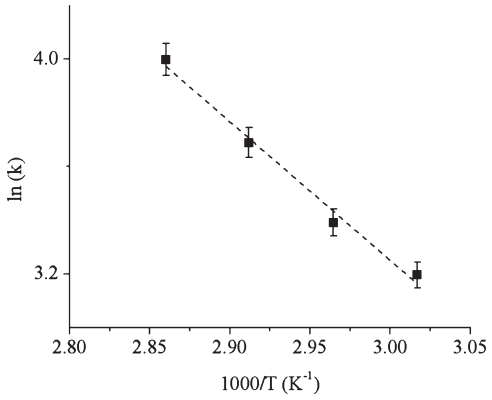

Figure 6. Arrhenius plot of ion exchange rates as a function of temperature for Li1−Li2 ion exchange in Li_2VPO_4F.

temperature range and mixing time period, are plotted beside the ^{6}Li 1D SI counterparts. Only the A resonance is evaluated because it was the environment chosen for selective inversion in the ^{6}Li 1D SI study. Figure 5 clearly shows that the initial portion of the EXSY buildup curves are influenced by changes in the ion dynamics while the NSI data remain relatively unchanged. This further confirms that thermally driven chemical exchange is taking place between the two Li environments of Li_2VPO_4F. The NSI data, however, cannot be taken as a true measurement of the inherent T_1 times of each environment. The T_1 values previously reported from the NSI experiments at 331 K (herein referred to as T_1^{NSI}) were 23 ± 1 and 18 ± 1 ms for spins A and B, respectively. By fitting the 1D EXSY data (also at 331 K) using CIFIT, a new set of T_1 values (abbreviated as T_1^{SI}) were generated. These values were determined from single component fits as the primary mechanism of relaxation in ^{6}Li MAS NMR is from dipolar coupling with the unpaired electrons sitting on the paramagnetic center. T_{1Q} and spin diffusion have negligible effects on these values.[33] For spins A and B, the fitted T_1^{SI} values of 29 ± 2 and 11 ± 1 ms, respectively, were determined. The T_1^{SI} is a more faithful representation of the inherent T_1 times of each environment in the absence of chemical exchange, which is further emphasized when the modeled T_1^{SI} values are compared with the experimentally measured T_1^{NSI} values. For the A spin, T_1^{SI} is longer than the T_1^{NSI}, whereas for the B spin, the opposite is true: the T_1^{SI} is shorter than the experimentally measured T_1^{NSI} value. This is a result of equilibration of the spin−lattice relaxation times for spins undergoing chemical exchange and further emphasizes how the T_1^{SI} values are a more accurate time scale of the spin−lattice relaxation in the absence of chemical exchange. The T_1^{SI} values were therefore held as a constant in the CIFIT models of ^{6}Li 1D EXSY data over the remaining variable temperature range.

Determination of jump rates for the Li1−Li2 exchange pair at different temperatures allowed for the calculation of the activation energy, E_a, as the natural log of the exchange rates was plotted as a function of inverse temperature in an Arrhenius plot (Figure 6). An energy barrier value of 0.44 ± 0.06 eV was calculated from the slope of the graph, where the error bounds on the $\ln(k)$ values were included in the regression analysis. The error value of the energy barrier was subsequently calculated from the standard error of the slope from the regression analysis. This activation energy was correlated to structural constraints within the lattice in a similar approach to previous studies, where

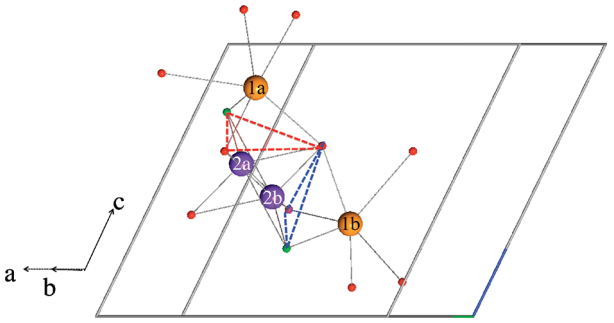

Figure 7. Schematic of the simplified unit cell highlighting the two face-shared Li1−Li2 (orange−lilac) diffusion pathways. Each has a bottleneck area (shaded triangle) created by 1 F atom (green) and 2 O atoms (red). Depending on the population of the half occupancy Li1 and Li2 environments, the α-bottleneck (red triangle) is present as either $\alpha 1$ (Li1a−Li2a) or $\alpha 2$ (Li1a−Li2b), Similarly, the β-bottleneck (blue triangle) exists as either $\beta 1$ (Li1b−Li2b) or $\beta 2$ (Li1b−Li2a). The coordination environments and pathways lend themselves to 3D ion transport.

Table 2. Summary of Face-Shared Li1−Li2 Pathways in Li_2VPO_4F with the Corresponding Bottlenecks for Diffusion and Internuclear Distances

Li1−Li2 pathway	area of bottleneck (Å^2)	Li1−Li2 distance (Å)
α_1	3.92	1.938
α_2	3.92	2.791
β_1	4.22	1.979
β_2	4.22	2.993

mechanisms of Li-transport were identified.[10,12,34] The lithiated−tavorite structure includes two crystallographically unique Li sites, both of which were previously determined to be half occupied.[5] Figure 7 shows a simplified unit cell, where the two pathways for Li-ion hopping are identified as face-shared geometries between the Li1−Li2 polyhedral environments. The bottlenecks for diffusion along each pathway were quantified by calculating the area of the triangular face created by the 2 O atoms and 1 F atom shared by the two exchanging Li sites. The first triangular window, which we term the α-bottleneck (red triangle, Figure 7), has a smaller area of 3.92 Å^2. The second triangular window, which we term the β-bottleneck (blue triangle, Figure 7), is more open with an area of 4.22 Å^2 (Table 2). The internuclear distances between the ions passing through the α and β bottlenecks, is complicated by the half-occupancy of the Li environments. For each bottleneck, there is one short and one long Li1−Li2 internuclear distance. For the case of the α bottleneck, the shorter Li1−Li2 distance of 1.938 Å is referred to as the α_1 pathway, whereas the longer 2.791 Å distance is the α_2 pathway (Table 2). Similarly for the β-bottleneck, β_1 identifies the Li1−Li2 distance of 1.979 Å, whereas β_2 indicates the pathway with a 2.993 Å Li1−Li2 distance. To minimize electrostatic repulsion between the Li environments, it is expected that the Li ions are separated by the longer internuclear distances in the structure. On the basis of this assumption, the two plausible exchange pathways occur such that the shorter internuclear distance is paired with the tighter bottleneck (α_2 pathway), as compared with the longer internuclear distance that is paired with the wider bottleneck (β_2 pathway). This makes differentiation

between these two possible pathways nontrivial, and the single rate determined here at each temperature is attributable to either of these exchange routes. Moreover, the similarity between the pathways, which are fitted to a single ion exchange rate for the 1D EXSY data at each temperature, is a strong indication of the propensity for 3D ion transport in this material.

CONCLUSIONS

This work presents the first quantitative study of Li^+ dynamics in tavorite Li_2VPO_4F. It also is the first quantitative study of ion dynamics in a solid-state paramagnetic system using 1D EXSY experiments. This is an example of a material where the spin−lattice relaxation rates are faster than the ion dynamics, and thus a 2D EXSY approach is nontrivial. Exchange between the two crystallographic Li sites was found to be on the millisecond time scale with an energy barrier of 0.44 ± 0.06 eV. Two pathways of ion exchange between Li1 and Li2 were identified, with similar structural constraints. This 1D EXSY method will be applicable for determining lithium ion dynamics in electrode materials and extended to materials with multiple lithium sites.

AUTHOR INFORMATION

Corresponding Author

*E-mail: goward@mcmaster.ca. Tel: (905)-525-9140, ext. 24176. Fax: (905)-522-2509.

REFERENCES

(1) Goodenough, J. B.; Kim, Y. *Chem. Mater.* **2010**, *22*, 587.
(2) Ellis, B. L.; Lee, K. T.; Nazar, L. F. *Chem. Mater.* **2010**, *22*, 691.
(3) Barker, J.; Gover, R. K. B.; Burns, P.; Bryan, A.; Saidi, M. Y.; Swoyer, J. L. *J. Power Sources* **2005**, *146*, 516.
(4) Barker, J.; Saidi, M. Y.; Swoyer, J. L. *J. Electrochem. Soc.* **2003**, *150*, A1394.
(5) Ellis, B. L.; Ramesh, T. N.; Davis, L. J. M.; Goward, G. R.; Nazar, L. F. *Chem. Mater.* **2011**, accepted .
(6) Nishimura, S.; Kobayashi, G.; Ohoyama, K.; Kanno, R.; Yashima, M.; Yamada, A. *Nat. Mater.* **2008**, *7*, 707.
(7) Jeener, J.; Meier, B. H.; Bachmann, P.; Ernst, R. R. *J. Chem. Phys.* **1979**, *71*, 4546.
(8) Xu, Z.; Stebbins, J. F. *Science* **1995**, *270*, 1332.
(9) Verhoeven, V. W. J.; de Schepper, I. M.; Nachtegaal, G.; Kentgens, A. P. M.; Kelder, E. M.; Schoonman, J.; Mulder, F. M. *Phys. Rev. Lett.* **2001**, *86*, 4314.
(10) Cahill, L. S.; Chapman, R. P.; Britten, J. F.; Goward, G. R. *J. Phys. Chem. B* **2006**, *110*, 7171.
(11) Davis, L. J. M.; Heinmaa, I.; Goward, G. R. *Chem. Mater.* **2010**, *22*, 769.
(12) Wilkening, M.; Romanova, E. E.; Nakhal, S.; Weber, D.; Lerch, M.; Heitjans, P. *J. Phys. Chem. C* **2010**, *114*, 19083.
(13) Cahill, L. S.; Chapman, R. P.; Kirby, C. W.; Goward, G. R. *Appl. Magn. Reson.* **2007**, *32*, 565.
(14) Forsen, S.; Hoffman, R. A. *J. Chem. Phys.* **1963**, *39*, 2892.
(15) Forsen, S.; Hoffman, R. A. *J. Chem. Phys.* **1964**, *40*, 1189.
(16) Alger, J. R.; Prestegard, J. H. *J. Magn. Reson.* **1977**, *27*, 137.
(17) Malloy, C. R.; Sherry, A. D.; Nunnally, R. L. *J. Magn. Reson.* **1985**, *64*, 243.
(18) Bain, A. D.; Cramer, J. A. *J. Magn. Reson., Ser. A* **1996**, *118*, 21.
(19) Grassi, M.; Mann, B. E.; Pickup, B. T.; Spencer, C. M. *J. Magn. Reson.* **1986**, *69*, 92.
(20) Perrin, C. L.; Engler, R. E. *J. Magn. Reson., Ser. A* **1996**, *123*, 188.
(21) Bain, A. D. *Prog. Nucl. Magn. Reson. Spectrosc.* **2003**, *43*, 63.
(22) Camara, J. M.; Petros, R. A.; Norton, J. R. *J. Am. Chem. Soc.* **2011**, *133*, 5263.
(23) De Crisci, A. G.; Annibale, V. T.; Hamer, G. K.; Lough, A. J.; Fekl, U. *Dalton Trans.* **2010**, *39*, 2888.
(24) Dunne, J. F.; Fulton, D. B.; Ellern, A.; Sadow, A. D. *J. Am. Chem. Soc.* **2010**, *132*, 17680.
(25) Jong, H.; Patrick, B. O.; Fryzuk, M. D. *Organometallics* **2011**, *30*, 2333.
(26) Kristian, K. E.; Limura, M.; Cummings, S. A.; Norton, J. R.; Janak, K. E.; Pang, K. *Organometallics* **2009**, *28*, 493.
(27) Moreno, A.; Pregosin, P. S.; Fuentes, B.; Veiros, L. F.; Albinati, A.; Rizzato, S. *Organometallics* **2009**, *28*, 6489.
(28) Szeverenyi, N. M.; Bax, A.; Maciel, G. E. *J. Am. Chem. Soc.* **1983**, *105*, 2579.
(29) Hampson, M. R.; Evans, J. S. O.; Hodgkinson, P. *J. Am. Chem. Soc.* **2005**, *127*, 15175.
(30) Srinivasan, S.; Magusin, P. C. M. M.; van Santen, R. A.; Notten, P. H. L.; Schreuders, H.; Dam, B. *J. Phys. Chem. C* **2011**, *115*, 288.
(31) Grey, C. P.; Cheetham, A. K.; Dobson, C. M. *J. Magn. Reson., Ser. A* **1993**, *101*, 299.
(32) Bain, A. D.; Berno, B. *Prog. Nucl. Magn. Reson. Spectrosc.* **2011**, 223–244.
(33) Xu, Z.; Stebbins, J. F. *Solid State Nucl. Magn. Reson.* **1995**, *5*, 103.
(34) Makimura, Y.; Cahill, L. S.; Iriyama, Y.; Goward, G. R.; Nazar, L. F. *Chem. Mater.* **2008**, *20*, 4240.